

NUMERICAL–EXPERIMENTAL INVESTIGATION OF THE ELASTIC DEFORMATION OF A POLYMERIC PIPELINE UNDER IMPACT

Yu. A. Kulikov,¹ Yu. V. Loskutov,¹
M. A. Maksimov,² and Yu. K. Zdanovich³

UDC 539.4

The paper reports results of numerical–experimental investigation of the hydroelastic process in a polyimide pipeline filled with a fluid. The propagation of small perturbations in the fluid is considered in an acoustic approximation based on wave equations. The equations are integrated using the method of characteristics and a two-layer difference scheme. The elastic problem is solved by the finite element method and the Newmark difference β -method. The stress–strain state of the pipeline is defined by a superposition of fast rod modes of motion and slow shell modes of motion. Satisfactory agreement between calculated and experimental data is obtained.

Introduction. Active control of hydraulic flows, which is typical of modern engineering constructions, is accompanied, as a rule, by development of wave hydrodynamic processes. The wave processes have a significant influence on the behavior of polymeric structures. Polymers are more compliant (deformable) than metals. As a result, the rate of perturbation propagation in a fluid decreases considerably, in particular, in pipes of a polyimide film, it decreases by a factor of more than 3 [1, 2]. When the time of perturbation is rather large, wave processes develop even in rather short pipes of this material, and this should be taken into account in structural analysis.

The goal of the present work was to study experimentally the hydroelastic process in a specimen of a polyimide pipeline filled with a fluid under impact and to develop a method for calculating the parameters of this process.

Computational Dynamic Model. In construction of a dynamic model, the hydraulic and mechanical systems are considered separately. It is assumed that the fluid is homogeneous, viscous, and incompressible and the perturbation is small. The problem of propagation of small perturbations in the fluid is solved in an acoustic approximation using a one-dimensional model and the wave equations

$$\frac{\partial p}{\partial t} + \rho_{\text{fl}} c_0^2 \frac{\partial v}{\partial x} = 0, \quad \frac{\partial v}{\partial t} + \rho_{\text{fl}}^{-1} \frac{\partial p}{\partial x} = -2Qv \quad (1)$$

with the initial conditions $p(x, 0) = 0$ and $v(x, 0) = 0$. Here $p(x, t)$ and $v(x, t)$ are the perturbations of pressure and velocity, x is the arc coordinate along the axial line, t is time, $c_0 = \sqrt{K_{\text{fl}} \{ \rho_{\text{fl}} [1 + 2K_{\text{fl}} r / (E h_m)] \}^{-1}}$ is the speed of wave propagation in the fluid, K_{fl} is the modulus of bulk elasticity of the fluid, E is the elastic modulus of the pipe material, ρ_{fl} is the density of the unperturbed fluid, Q is the hydraulic resistance (calculated in a quasistationary approximation by the Darcy–Weisbach formula [3]), r is the average cross-sectional radius, and h_m is the rated wall thickness. Equations (1) take into account the elastic deformation of the wall and the

¹Mari State Technical University, Yoshkar Ola 424024. ²Research Institute of Special Mechanical Engineering of the Bauman Moscow State Technical University, Moscow 107005. ³Designer Bureau “Salute” of the Khrunichev State Space Research-and-Production Center, Moscow 121087. Translated from *Prikladnaya Mekhanika i Tekhnicheskaya Fizika*, Vol. 42, No. 2, pp. 122–128, March–April, 2001. Original article submitted January 10, 2000; revision submitted September 18, 2000.

compressibility of the fluid. The influence of the channel curvature and the initial geometrical irregularities on the speed of propagation of acoustic waves is ignored.

Integration of the differential hyperbolic equations (1) is performed by the method of characteristics [3]. A regular difference grid is constructed on the characteristics in the plane (x, t) . The interval of integration $[0, L]$ is divided into n of segments with step $\Delta x = L/n$. The step Δx corresponds to the time step $\Delta t = \Delta x/c_0$. The differential equations (1) are written in finite differences:

$$\begin{aligned} p_{i,k+1} - p_{i,k} + \rho_{fl} c_0 (v_{i,k+1} - v_{i,k}) + \rho_{fl} Q_{i,k} v_{i,k} (x_{i,k+1} - x_{i,k}) &= 0, \\ p_{i,k+1} - p_{i+1,k} - \rho_{fl} c_0 (v_{i,k+1} - v_{i+1,k}) + \rho_{fl} Q_{i+1,k} v_{i+1,k} (x_{i,k+1} - x_{i+1,k}) &= 0, \end{aligned} \quad (2)$$

$$i = \begin{cases} 1, 2, \dots, n+1 & \text{for } k = 1, 3, 5, \dots, \\ 1, 2, \dots, n & \text{for } k = 2, 4, 6, \dots \end{cases}$$

The subscripts k and i denote the time layer and the axial coordinate of the points of intersection of the characteristics, respectively.

The solution of Eqs. (1) should satisfy the following boundary conditions: $p(0, t) = p(t)$ at the pipe entrance and $v(L, t) = 0$ at the exit. The function $p(t)$ defines the pressure variation due to mechanical impact of a piston (measured experimentally). Using the value of one parameter (at the entrance or exit) from Eqs. (2), we obtain the other parameter:

$$\begin{aligned} p_{1,k+1} = p(t_k + \Delta t/2), \quad v_{1,k+1} = v_{2,k} + \frac{p_{1,k+1} - p_{2,k}}{\rho_{fl} c_0} - \frac{\Delta x Q_{2,k} v_{2,k}}{c_0} \quad \text{for } x = 0, \\ v_{n+1,k+1} = 0, \quad p_{n+1,k+1} = p_{n,k} + \rho_{fl} c_0 v_{n,k} - \rho_{fl} \Delta x Q_{n,k} v_{n,k} \quad \text{for } x = L, \quad k = 2, 4, 6, \dots \end{aligned}$$

The nonstationary problem of dynamics is solved by the finite element method. The behavior of the pipeline is described by the system $[M]\{\ddot{q}\} + [B]\{\dot{q}\} + [C]\{q\} = \{F(t)\}$. Here $[M]$, $[C]$, and $[B] = \chi_1[C] + \chi_2[M]$ are the mass, stiffness, and damping matrices, respectively, $\{q\}$, $\{\dot{q}\}$, and $\{\ddot{q}\}$ are the generalized displacement, velocity, and acceleration vectors, respectively (points denote differentiation with respect to time), χ_1 and χ_2 are Rayleigh parameters, and $\{F(t)\}$ is the hydrodynamic load vector. It is assumed that the material is homogeneous and isotropic and the displacements and strains are small.

The curvilinear pipeline is simulated by an ensemble of nine finite elements (FE) with 48 degrees of freedom and is treated as a bound shell-rod system. The stress-strain state is determined by a superposition of fast rod modes of motion and slow shell modes of motion. In the consideration of the shell modes, the inertial force and resistance to motion are ignored.

The oscillations modes of a curvilinear FE are approximated by two systems of basis functions [4, 5]. One system describes the oscillations of the FE as a rod. The terms corresponding to the rigid displacement of the FE are

$$\begin{aligned} u_1(s, t) = \alpha_7 \sin \phi - \alpha_8 R \cos \phi, \quad v_1(s, t) = \alpha_4 R \sin \phi + \alpha_{11} R \cos \phi, \\ w_1(s, t) = \alpha_7 \cos \phi + \alpha_8 R \sin \phi, \quad \varphi_1(s, t) = \alpha_4 \sin \phi + \alpha_{11} \cos \phi, \end{aligned} \quad (3)$$

and the terms due to elastic deformation are

$$\begin{aligned} u_2(s, t) = \alpha_1 + \alpha_2 \phi + \alpha_9 \phi \cos \phi + \alpha_{10} \phi \sin \phi, \quad v_2(s, t) = \alpha_3 + \alpha_5 R \phi \cos \phi + \alpha_6 \phi + \alpha_{12} R \phi \sin \phi, \\ w_2(s, t) = -\alpha_9 (\phi \sin \phi + a \cos \phi) + \alpha_{10} (\phi \cos \phi - a \sin \phi), \\ \varphi_2(s, t) = \alpha_5 (\phi \cos \phi + b \sin \phi) + \alpha_{12} (\phi \sin \phi - b \cos \phi). \end{aligned} \quad (4)$$

Here $u = u_1 + u_2$, $v = v_1 + v_2$, and $w = w_1 + w_2$ are the axial, normal, and radial components of the vector of displacement of the center of gravity, respectively, $\varphi = \varphi_1 + \varphi_2$ is the rotation angle of the cross section, $\alpha_i(t)$ ($i = 1, 2, \dots, 12$) are the generalized coordinates, ϕ is the angular coordinate $[-\phi_0/2 \leq \phi \leq \phi_0/2]$, where ϕ_0 is the central angle (pipe bending angle)], and a and b are dimensionless coefficients.

Another system of coordinate functions describes the oscillations of the FE as a thin shell (the Kármán effect and manometric effect). In this case, it is assumed that

$$w(\phi, \theta, t) = \sum_{m=0}^1 \sum_{n=2}^N (w_{1,mn} \cos(n\theta) + w_{2,mn} \sin(n\theta)) \cos(m\pi\phi/\phi_0), \quad (5)$$

where w is the radial displacement of points on the shell midsurface, $N = 8$ is the number of harmonics in the solution expansion in the circumferential coordinate θ , and $w_{1,mn}(t)$ and $w_{2,mn}(t)$ are generalized coordinates that correspond to symmetric and skew-symmetric modes, respectively. The symmetric modes describe the bend in the plane of pipe curvature, and the skew-symmetric modes describe the bend in a perpendicular plane.

The required system of linear algebraic equations [6] is constructed using the variational Lagrange equation and the Vlasov semimomentless theory of thin shells.

The oscillation modes of a rectilinear FE as a rod are approximated by algebraic polynomials [7].

Approximations (3) and (4) are used to build up the stiffness and mass (12×12) matrices of the FE:

$$[C^n] = \int_L [\Phi]^t [H]^t [D] [H] [\Phi] ds, \quad [M^n] = \int_L [\Phi]^t [m] [\Phi] ds, \quad [D] = \text{diag} [EA, 2GI, EI/k, EI/k],$$

$$[H] = \begin{bmatrix} d/ds & 0 & -1/R & 0 \\ 0 & -d/Rds & 0 & d/ds \\ d/Rds & 0 & d^2/ds^2 & 0 \\ 0 & -d^2/ds^2 & 0 & -1/R \end{bmatrix}, \quad (6)$$

$$[m] = \text{diag} [m_p, m_p + m_{fl}, m_p + m_{fl}, I_p].$$

Here n is the ordinal number FE, $s = R\phi$ is the arc coordinate, L is the length of the FE, $[H]$ is the differential operator matrix, $[\Phi]$ is the approximating function (shape function) matrix, m_p and m_{fl} are the masses of the pipe and the attached fluid per unit length, I_p is the moment of inertia of the mass m_p relative to the pipe axis, G is the shear modulus, A and I are the area and moment of inertia of the cross section, and k is the ratio of the compliances of the curvilinear and rectilinear pipes [calculated from (5)].

For a curvilinear FE, the coefficients of the matrices $[C^n]$ and $[M^n]$ are calculated by the Gauss scheme. As $1/R \rightarrow 0$ and $k \rightarrow 1$, expressions (6) correspond to a rectilinear FE. In this case, integrals (6) are taken analytically.

The components of the vector $\{F(t)\}$ are determined, according to the displacement method, as the responses of nodal connections taken with the opposite sign [8]. For a two-node FE, we have

$$\begin{Bmatrix} F_i^n(t) \\ F_j^n(t) \end{Bmatrix} = - \begin{bmatrix} C_{ii}^n \\ C_{ji}^n \end{bmatrix} \{\Delta_{i1}^n(t) + \Delta_{i2}^n(t)\} + \begin{Bmatrix} 0 \\ Y_j^n(t) \end{Bmatrix}. \quad (7)$$

Here i and j are the node numbers, C_{ii}^n and C_{ji}^n are the stiffness submatrices of the FE (6×6), $Y_j^n(t)$ is the vector of node responses to the friction of the fluid against the pipe wall, $\Delta_{i1}^n(t)$ and $\Delta_{i2}^n(t)$ are the vectors of generalized displacements of the free node i (the node j is clamped). The elastic displacements $\Delta_{i1}^n(t)$ are due to the pressure $p(t)$ and velocity head $\rho_{fl}v^2(t)/2$, and the displacements $\Delta_{i2}^n(t)$ are due to the friction and manometric effect. The internal pressure unbends the curvilinear segments of the pipe having initial ovality and different wall thickness, and as a result, deforms the entire pipeline. The components of the vector $\Delta_{i2}^n(t)$ are calculated in [9].

The system of equations is integrated by the finite element method using the one-step algorithm of the Newmark β -method [10]. It is assumed that $\{q\} = \{\dot{q}\} = 0$ for $t = 0$. In each time step, the fluid parameters are calculated using relations (2) and the hydrodynamic load vector (7) is formed.

Description of Experiment. The laboratory setup designed for investigation of the hydroelastic process is shown schematically in Fig. 1, where 1 is the pipeline specimen, 2 is the loading hydrocylinder, 3

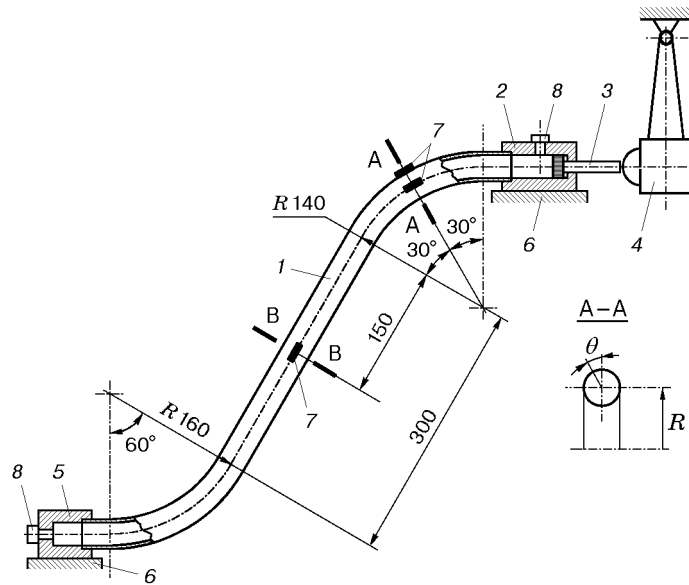


Fig. 1

is the piston, 4 is the pendulum impactor, 5 is the plug, 6 is the frame, 7 are the strain gages, and 8 are the pressure gauges.

The pipeline specimen is a thin-walled curvilinear pipe produced by winding of a polyimide film $50 \mu\text{m}$ thick. The specimen has the following dimensions: average cross-sectional radius $r = 20 \text{ mm}$, rated wall thickness $h_m = 1.5 \text{ mm}$, length of the axial line $L = 624 \text{ mm}$, amplitude of the initial irregularities of the cross-sectional shape $\Delta = (d_{\text{max}} - d_{\text{min}})/4 = 0.5 \text{ mm}$ (d_{max} and d_{min} are the diameters measured on the curvilinear segments over the external surface of the pipe in the plane of curvature and in a perpendicular plane). The physicomaterial characteristics of the material are as follows: elastic modulus $E = 3.2 \text{ GPa}$, Poisson's coefficient $\nu = 0.4$, and density $\rho_p = 1.47 \text{ g/cm}^3$.

The loading device is a pendulum impactor with a hammer having 12 steps of "cock" to govern the impact momentum. For a constant momentum, the impact strength is governed by a spring attached to the piston of the hydrocylinder.

The pipeline specimen, the hydrocylinder, and the plug are made fast to the impactor frame. The position is chosen so that the axis of the piston and the hydrocylinder coincides with the tangent to the trajectory of motion of the impactor hammer.

Measurements and recording of results are performed using 2PKB-10-200B strain gages, LKh-412 pressure gauges, a bridge block, an LKh-7000 strain station, and S9-8 digital memory oscillographs. The strain gauges are stick to the specimen by a cyacryn adhesive. In the hydrocylinder and plug there are screw ports to install the pressure gauges.

The interior of the pipe is filled with water. To prevent penetration of air and formation of gas bubbles, the filling port is made in the upper part of the hydrocylinder.

The experimental technique includes calibration of the measuring channels and the measurement procedure itself. The strain measuring channels are calibrated using reference resistances. The pressure channels are calibrated by loading the system at constant pressure. The measurement error for pressure and linear strains does not exceed 3%.

Comparative Analysis of Results. Results of the numerical-experimental investigation are given in Figs. 2 and 3 (curves are experimental results and points are calculated data). Figure 2a and Fig.2b show the pressure variation at the pipe entrance and exit, respectively, under mechanical impact of the piston. The peaks in the plots are explained by wave processes and are due to wave propagation and reflection in the fluid. The time over which the wave travels the total pipe length $\tau = 1.88\text{--}2.2 \text{ msec}$ is determined experimentally as the delay of the wave (Fig. 2b).

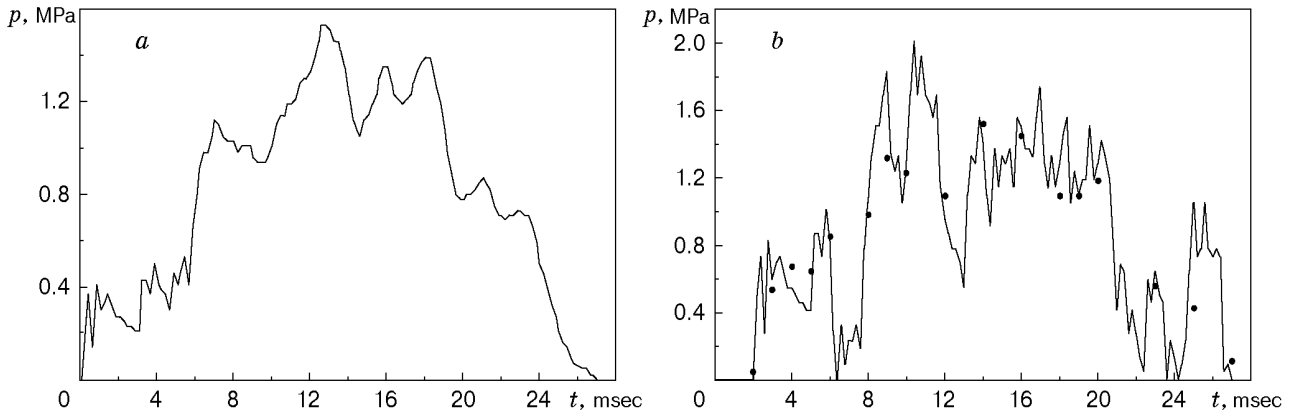


Fig. 2

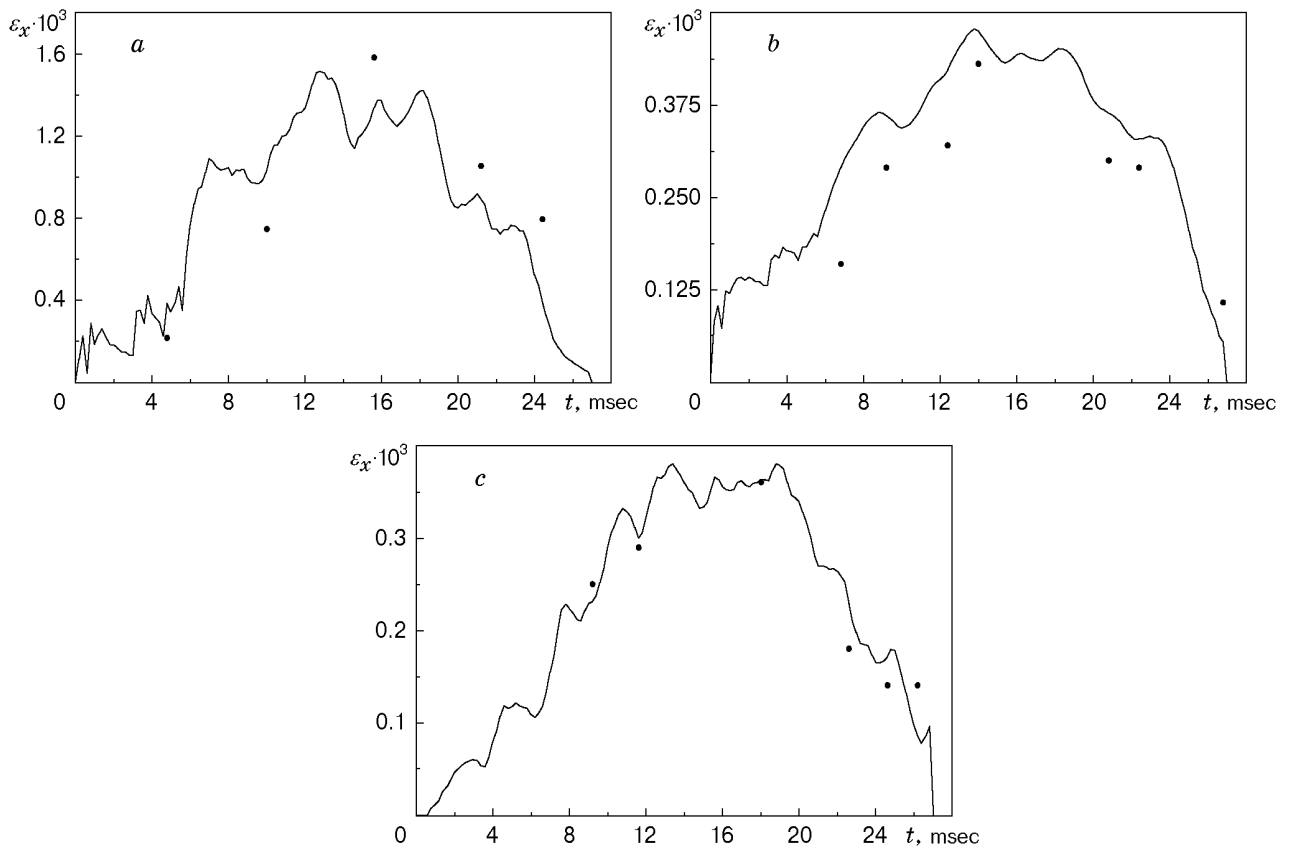


Fig. 3

The propagation speed of pressure waves calculated with allowance for the compliance of the wall is $c_0 = 298$ m/sec. In the case of an absolutely rigid wall, $c_0 = 1472$ m/sec (i.e., because of the elasticity of the wall material, the velocity c_0 decreases by a factor of about 5). The velocity c_0 corresponds to the time $\tau = L/c_0 = 2.09$ msec. Thus, the calculated and experimental values of τ are in good agreement.

In Fig. 2b, the pressure calculated for individual times according to (2) is compared to experimental data. The calculations are performed with the steps $\Delta t = 0.2$ msec $\approx 0.1\tau$ and $\Delta x = \Delta t c_0 = 5.96$ cm. From Fig. 2b it follows that the calculation data agree with the experimental data.

The calculated values for the six lowest eigenfrequencies ω_i of the pipeline with a fluid are $\omega_1^* = 61.9$ Hz, $\omega_2 = 63.1$ Hz, $\omega_3^* = 139$ Hz, $\omega_4 = 235$ Hz, $\omega_5^* = 256$ Hz, and $\omega_6^* = 294$ Hz (asterisk denotes the frequencies of oscillations in a direction perpendicular to the plane of pipe curvature). These frequencies range from 61.9 to 294 Hz. At the same time, the eigenfrequencies calculated for an individual FE and corresponding to shell modes (radial and flexural motions of the wall [9]) exceed 580 Hz. The frequency of pressure fluctuations is $\omega = 1/(4\tau) = 120$ Hz. In view of this, for the rod modes (3) and (4), the pressure is treated as a dynamic load, and for the shell modes (5), it is treated as a quasistatic load.

Figure 3 shows curves of the axial strain ε_x versus time. The axial strains were measured at points with the coordinates $\theta = 0$ (Fig. 3a) and $\theta = 90^\circ$ (Fig. 3b) in the section A–A on the external surface of the pipe and at points with the coordinates $\theta = 90^\circ$ in the section B–B (Fig. 3c). (The angle θ is shown in Fig. 1.) The calculations were performed for Rayleigh parameters $\chi_1 = 1.75 \cdot 10^{-3}$ and $\chi_2 = 8.45 \cdot 10^{-3}$, which were computed according to [10]. The logarithmic decrement $\delta = 0.032$ was determined experimentally on tubular polyimide specimens by the damped free oscillation technique.

An analysis of the results shows that for the curvilinear segment of the pipe, the difference between the calculated strains ε_x and the experimental values is not more than 30% (Fig. 3a and b), and for the rectilinear segment, it is not more than 7% (Fig. 3c). Thus, the calculation results are in satisfactory agreement with experimental data.

It should be noted that at points with $\theta = 90^\circ$ located in the plane of symmetry of the curvilinear segment (Fig. 3b) and at points with $\theta = 90^\circ$ on the rectilinear segment of the pipe (Fig. 3c), the axial strains are close to the strains in the momentless state. At the same time, at the point on the external surface of the curvilinear segment with $\theta = 0$ (Fig. 3a), the axial strains are about 5 times larger than the strains in the momentless state. This is apparently related to the bending of the wall due to the initial geometrical irregularities of the curvilinear segments of the pipe.

REFERENCES

1. E. N. Nekhoroshikh, V. M. Kuznetsov, and V. A. Shishatskii, "Polymer film materials in cryogenic pipeline mains," in: *Space-Rocket Engineering: Fundamental Problems of Mechanics and Heat Exchange*, Abstracts of the Int. Sci. Conf. (Moscow, November 10–11, 1998) [in Russian], Izd. Mosk. Tekh. Univ., Moscow (1998), pp. 176.
2. Yu. A. Kulikov, Yu. V. Loskutov, M. A. Maksimov, and Yu. K. Zdanovich, "Numerical–experimental investigation of the hydrodynamic loading and deformation of cryogenic pipelines made of polyimide materials," in: *Space Technique and Advanced Technologies-2000*, Abstracts All-Union Sci. Conf. (Perm', April 12–14, 2000) [in Russian], Izd. Perm. Tekh. Univ., Perm' (2000), p. 113.
3. I. A. Charnyi, *Unsteady Motion of a Real Fluid in Pipes* [in Russian], Nedra, Moscow (1975).
4. Yu. A. Kulikov, "Stress–strain state of a pipeline under hydraulic impacts," *Probl. Mashinostr. Nadezh. Mashin*, No. 3, 43–50 (1999).
5. V. I. Zaplatin, Yu. A. Kulikov, and I. V. Stasenko, "Analysis of a computational dynamic model for a thin-walled spatial pipeline," in: *Building Structures and Mechanics of a Solid Deformable Body* (collected papers) [in Russian], No. 1, Izd. Mariisk. Tekh. Univ. (1998), pp. 60–69.
6. I. V. Stasenko, *Creep Analysis of Pipelines* [in Russian], Mashinostroenie, Moscow (1986).
7. V. A. Postnov and I. Ya. Kharkhurim, *Finite Element Method in Ship Structure Designs* [in Russian], Sudostroenie, Leningrad (1974).
8. Yu. A. Kulikov, "Fluid pipelines: Numerical investigation of the stress–strain state induced by a stationary internal flow," in: *Strength Analysis* (collected papers) [in Russian], No. 33, Mashinostroenie, Moscow (1993), pp. 119–131.
9. Yu. A. Kulikov, "Influence of initial technological irregularities on the vibration of thin-walled curvilinear pipes with internal pressure fluctuations," in: *Probl. Mashinostr. Nadezh. Mashin*, No. 6, 11–21 (1993).
10. K.-J. Bathe and E. L. Wilson, *Numerical Methods in Finite Element Analysis*, Prentice-Hall, Englewood Cliffs, NJ (1976).